

Article

Discovery of Novel Indolealkylpiperazine Derivatives as Potent 5-HT_{1A} Receptor Agonists for the Potential Future Treatment of Depression

Chen Zhu, Xinwei Li, Weiqing Peng and Wei Fu *

Department of Medicinal Chemistry, School of Pharmacy, Fudan University, 826 Zhangheng Road, Pudong New District, Shanghai 201203, China; 18211030013@fudan.edu.cn (C.Z.); 19211030070@fudan.edu.cn (X.L.); 15211030063@fudan.edu.cn (W.P.)

* Correspondence: wfu@fudan.edu.cn

Received: 26 August 2020; Accepted: 1 October 2020; Published: 1 November 2020



Abstract: Depression is a severe psychiatric disorder that affects over 100 million people worldwide. 5-HT_{1A} receptor agonists have been implicated in the treatment of a variety of central nervous system diseases, especially depression. In this study, based on **FW01**, a selective potent 5-HT_{1A}R agonist discovered via dynamic pharmacophore-based virtual screening, a series of indolealkylpiperazine derivatives with a benzamide moiety were designed and synthesized by the modification of the amide tail group as well as indole head group of **FW01**. Among all tested compounds, **13m** displayed potent agonistic activity towards 5-HT_{1A}R with an EC₅₀ value of 1.01 nM. Molecular docking studies were performed to disclose the mechanism of its potent agonistic activity and high selectivity. Finally, the activation model of 5-HT_{1A}R induced by **13m** was proposed.

Keywords: 5-HT_{1A} receptor agonist; depression; drug design; molecular dynamics

1. Introduction

Depression is a severe psychiatric disorder that affects over 100 million people worldwide [1]. The main symptoms include low mood, lack of energy, sadness, insomnia, etc. [2]. Patients also suffer a high risk of suicide [3,4]. Though the etiology of depression is not clear, it is certain that genetic and psychological factors as well as environmental factors are all involved in the pathogenesis [5,6]. Selective serotonin reuptake inhibitors (SSRIs) and serotonin norepinephrine reuptake inhibitors (SNRIs) are common antidepressants clinically [7–9]. Though SSRIs are first-line drugs for the treatment of depression, they still have some drawbacks including delayed onset and limited efficacy [10,11]. Thus, drug discovery for new antidepressants with rapid onset and good efficacy is still urgent [12,13].

Serotonin (5-hydroxytryptamine, 5-HT), as an important neurotransmitter, is involved in multiple physiological and behavioral processes [14,15]. 5-HT mediates its physiological effects through at least 14 different receptor subtypes [16]. Among them, 5-HT_{1A} receptor (5-HT_{1A}R) plays a significant role in mood regulation and has been a hot target for various central nervous system disorders, especially depression [17–20]. Medicines like gepirone, tandospirone and vilazodone acting as 5-HT_{1A}R partial agonists are representative antidepressants clinically [21]. Meanwhile, the combination of 5-HT_{1A}R agonists and SSRIs not only accelerate the onset of SSRIs but also improve the therapeutic effect [10]. Therefore, based on our previous research, we aimed at discovering selective 5-HT_{1A}R agonists with novel scaffold with the eventual aim to treat depression.

2. Results and Discussion

2.1. Compound Design

In our previous study, a series of lead compounds as 5-HT_{1A}R agonists with novel scaffolds were obtained through the combination of pharmacophore-based virtual screening and biological assay [22]. Among them, **FW01** (Figure 1) possessed high activity for 5-HT_{1A}R ($K_i = 51.9 \pm 16.4$ nM), medium activity for 5-HT_{2A} receptor (5-HT_{2A}R) ($K_i = 206.71 \pm 7.46$ nM) and low activity for dopamine D₂ receptor (D₂R) ($K_i = 2161.35 \pm 25.55$ nM). **FW01** was bound to 5-HT_{1A}R via multiple interaction forces [22].

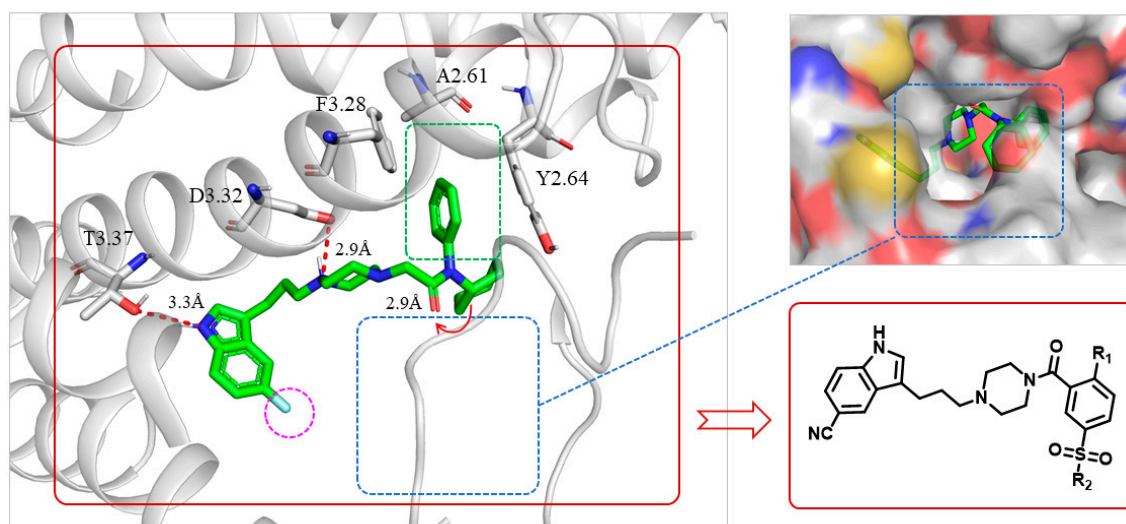


Figure 1. Predicted binding mode of **FW01** (green sticks) with 5-HT_{1A}R (cartoon) and the design of indolealkylpiperazine derivatives. Ligands are shown as green sticks. The binding residues of 5-HT_{1A}R are shown in gray. Hydrogen bond interactions are represented as dotted red lines. 5-HT_{1A}R was obtained by homology modeling from the X-ray structure of 5-HT_{1B}R (PDB code: 6G79).

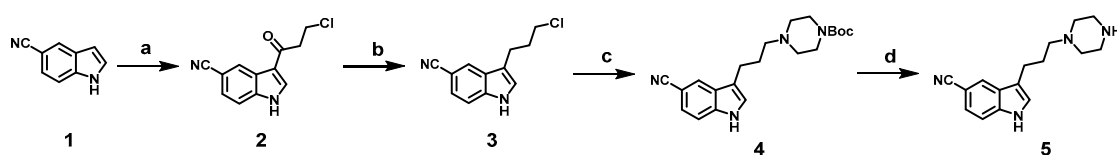
The docking predicted binding mode of **FW01** with 5-HT_{1A}R (Figure 1) showed that the indole head group was inserted into the pocket formed by transmembrane helix 3 (TM3), TM5, TM6 and TM7 of 5-HT_{1A}R. The NH group of the indole head formed hydrogen bonding with T3.37. The protonated nitrogen of piperazine participated in the salt bridge with D3.32. As for the amide tail group, the phenyl ring was inserted into the pocket formed by residues F3.28, Y2.64, and A6.21. However, there was an empty pocket formed by TM6 and TM7 which was not reached by **FW01**. Due to the presence of the upper pocket and the lower pocket formed by TM6 and TM7, the amide tail moiety of **FW01** was replaced with different 2,5-substituted benzamide moieties. As for the indole moiety, the development of marketed antidepressant drug vilazodone showed that a 5-CN indole moiety could enhance the 5-HT_{1A}R affinity, which was also proved in our previous study [23,24]. Therefore, the 5-F indole moiety of **FW01** was replaced by 5-CN indole moiety to raise the agonistic activity of designed compounds towards 5-HT_{1A}R.

Finally, a series of indolealkylpiperazine derivatives with a benzamide moiety were designed and synthesized. Their cellular function activities on dopamine and serotonin receptors were evaluated by Ultra Lance cAMP assay and Fluorometric Imaging Plate Reader (FLIPR) assay.

2.2. Chemical Synthesis

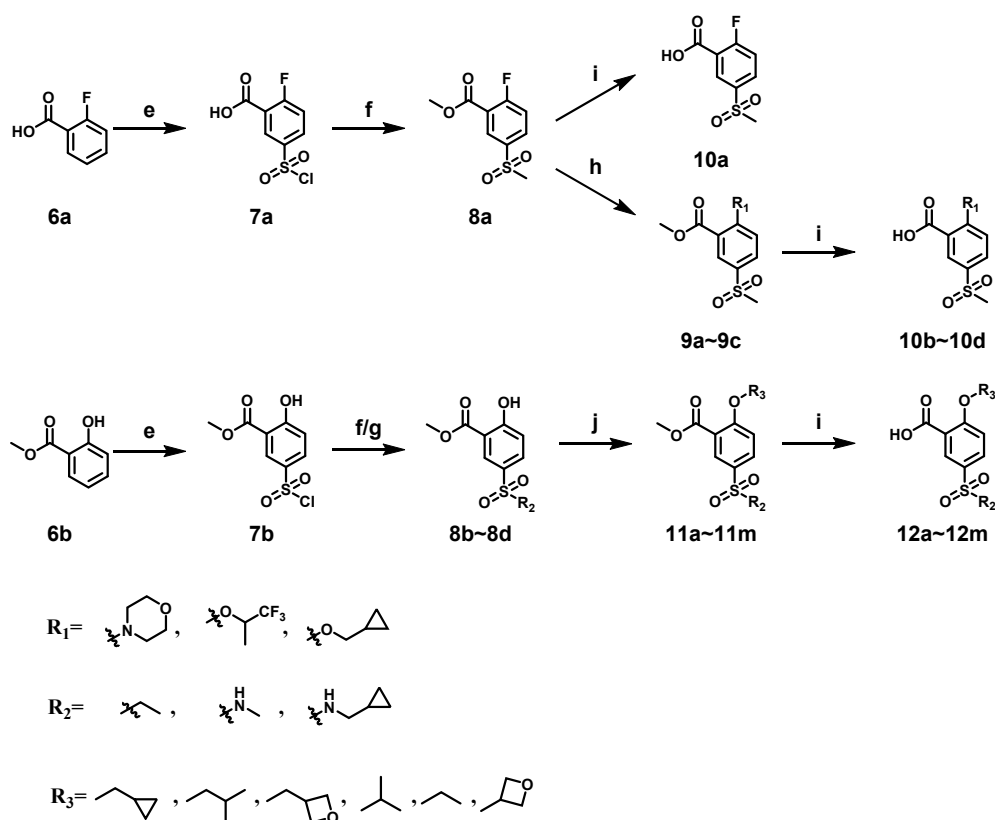
Synthesis of intermediate **5** was shown in Scheme 1. Commercially available 5-cyanoindole was first acylated with 3-chloropropionyl chloride via Friedel-Crafts acylation to obtain **2**, which was

reduced by $\text{NaBH}_4/\text{CF}_3\text{COOH}$ system to give compound **3**. Compound **4**, which was obtained via the reaction of **3** and N-Boc-piperazine, was deprotected to give **5**.



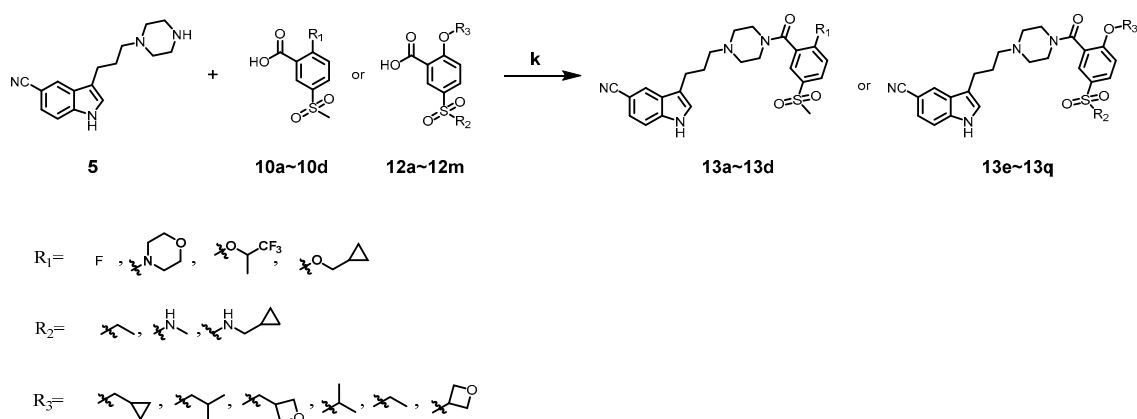
Scheme 1. Synthesis of intermediate **5**. Reagents and conditions: (a) 3-chloropropionyl chloride, AlCl_3 , anhydrous DCM, r.t., overnight; (b) NaBH_4 , CF_3COOH , anhydrous THF, 0°C , 1 h; (c) Boc-piperazine, CH_3CN , K_2CO_3 , 75°C , 36 h; (d) CF_3COOH , DCM, r.t., 4 h.

Synthesis of the 5-sulfonyl benzoic acid was outlined in Scheme 2. Compound **7a** was obtained by the sulfonation reaction of **6a** and chlorosulfonic acid. **7a** reacted with sodium sulfite and then alkylated by iodomethane to give **8a**. **8a** was deprotected by lithium hydroxide to give **10a**. Synthesis of **10b–10d** was accomplished by reaction of **8a** and corresponding reagents and then deprotection by lithium hydroxide. For **8b–8d**, the starting material was methyl salicylate and the synthetic route was similar to **8a**. Compounds **11a–11m** were obtained by Mitsunobu reaction of **8b–8d** and corresponding alcohol or alkylation of **8b–8d** and 3-iodo-oxetane, which were then deprotected by lithium hydroxide to give compounds **12a–12m**.



Scheme 2. Synthesis of benzoic acid intermediates. Reagents and conditions: (e) HClSO_3 , 40°C , 30 min; (f) i. Na_2SO_3 , H_2SO_4 , H_2O , r.t., 2 h; ii. iodide alkanes, K_2CO_3 , DMF, r.t., 3 h; (g) amine, DCM, r.t., 2 h; (h) corresponding reagent, K_2CO_3 , DMF, 150°C , 18 h; (i) $\text{LiOH}\cdot\text{H}_2\text{O}$, $\text{THF}:\text{H}_2\text{O} = 4:1$, r.t., 5 h; (j) alcohol, PPh_3 , DBAD, THF, r.t., 6 h or 3-iodo-oxetane, Cs_2CO_3 , DMF, 80°C , 10 h.

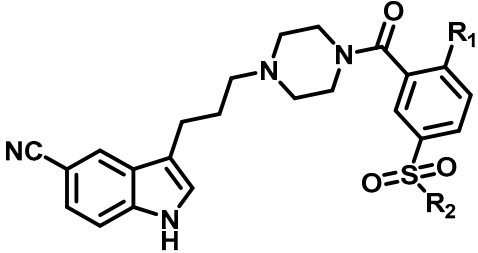
As shown in Scheme 3, compounds **13a–13q** were obtained by condensation of **5** and benzoic acid intermediate. Structure of all compounds were confirmed by ESI-MS, HRMS, ^1H NMR and ^{13}C NMR.

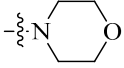
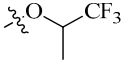
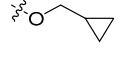
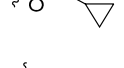
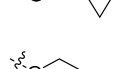
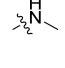

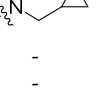


Scheme 3. Synthesis of compounds **13a–13q**. Reagents and conditions: (k) EDC·HCl, HOBT, DIEA, DCM, r.t., 8 h.

2.3. In Vitro Biological Activity Evaluation

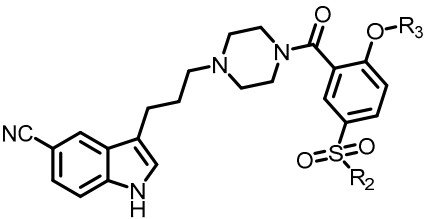
After these new derivatives were synthesized, they were all subjected to in vitro evaluation of functional activities towards 5-HT_{1A}, 5-HT_{2A} and D₂ receptors. As shown in Table 1, indolealkylpiperazine derivatives displayed varied selectivity for 5-HT_{1A}R over D₂R and 5-HT_{2A}R. When R₂ was methyl group, R₁ was subjected to substituents of different size to examine the SAR. Compound **13a** with an F atom displayed reduced agonistic activity for 5-HT_{1A}R. The introduction of morpholine group (**13b**) resulted in drastically decreased activity towards three receptors, indicating that large size group of R₁ position was not compatible with these receptors. Replacing morpholine group with smaller size 1,1,1-trifluoro-2-propyl or cyclopropylmethoxy group afforded **13c** and **13d**, respectively. By comparing **13b**, they showed increased activity for 5-HT_{1A}R and 5-HT_{2A}R. We postulated that the cyclopropylmethoxy group extended into the hydrophobic pocket where the phenyl ring of FW01 located, thus stabilizing the binding conformation of **13d** in the active pockets of 5-HT_{1A}R and 5-HT_{2A}R. Then, the ethyl, methylamino and cyclopropylmethylamino groups were employed to replace methyl of **13d** and compounds **13e–13g** were designed. When adopting the sulfonamide substituents (**13f** and **13g**), the activity for 5-HT_{1A}R showed a remarkable elevation in comparison to compound **13a–13e**, presumably due to the less flexible nitrogen chain posing a limited conformation to form a more stable hydrophobic interaction.

Table 1. Functional activities of compounds **13a–13g** for dopamine receptor (D₂R) and serotonin receptors (5-HT_{1A}R and 5-HT_{2A}R).


Compound	R ₁	R ₂	D ₂ R	5-HT _{1A} R	5-HT _{2A} R
			IC ₅₀ (nM)	EC ₅₀ (nM)	IC ₅₀ (nM)
FW01	-	-	2161.35 ± 25.55 ^a	7	206.71 ± 7.46 ^a
13a	-F	-CH ₃	NA	167.7	>5000
13b		-CH ₃	NA	989.7	NA
13c		-CH ₃	NA	197.2	1144
13d		-CH ₃	NA	88.0	887.4
13e		-CH ₂ CH ₃	>5000	49.2	1292
13f			NA	23.6	1099
13g			4311	5.35	2277
Risperidone	-	-	2.6	-	3.2
8-OH-DPAT	-	-	-	7.3	-

a: K_i value; NA: no activity.

Encouraged by the results above, we next extended our efforts to investigate the effect of substituents of position 2 of the phenyl ring on compounds **13f** and **13g**. Overall, compounds **13f–13q** showed selective agonistic activity for 5-HT_{1A}R. Among these compounds, **13g** and **13m–13q** bearing cyclopropylmethylamino moiety displayed more potent activity for 5-HT_{1A}R than their corresponding compounds **13f** and **13h–13l** bearing methylamino moiety, suggesting that cyclopropylmethylamino moiety was more favorable than methylamino moiety at position 2 as shown in Table 2. Compounds **13h** and **13m** bearing the isobutyl moiety were found to demonstrate the most potent agonistic activity for 5-HT_{1A}R among methylamine and cyclopropylmethylamino moiety possessing compounds, respectively. Compound **13j** with isopropyl group was found to completely lose activity for 5-HT_{1A}R, which was due to the isopropyl moiety of **13j** forming steric hindrance with 5-HT_{1A}R. As for **13o** which showed potent activity for 5-HT_{1A}R, the presence of the N-(cyclopropylmethyl)sulfamoyl moiety limited the conformation of the compound. By contrast, the introduction of a polar atom to the R₃ group resulted in a decreased activity for 5-HT_{1A}R by an order of magnitude, indicating that a polar group was unfavorable to the binding affinity towards 5-HT_{1A}R (**13i**, **13l**, **13n**, **13q**).

Table 2. Functional activities of compounds **13f–13q** for dopamine receptor (D₂R) and serotonin receptors (5-HT_{1A}R and 5-HT_{2A}R).


Compound	R ₂	R ₃	D ₂ R	5-HT _{1A} R	5-HT _{2A} R
			IC ₅₀ (nM)	EC ₅₀ (nM)	IC ₅₀ (nM)
13f			NA	23.6	1099
13h			NA	5.67	567.4
13i			NA	400.5	4186
13j			NA	NA	NA
13k			NA	77.5	1778
13l			NA	523.9	NA
13g			4311	5.35	2277
13m			>5000	1.01	1528
13n			NA	31.6	>5000
13o			NA	22.8	NA
13p			NA	48.2	4730
13q			NA	174.7	NA
Risperidone	-	-	2.6	-	3.2
8-OH-DPAT	-	-	-	7.3	-

NA: no activity.

2.4. Binding Mode

We next studied the binding mode of **13m** with agonistic conformation of 5-HT_{1A}R. We used the GOLD 5.1 program to dock **13m** into the binding site of the 5-HT_{1A}R which was obtained by homology modeling from the X-ray structure of 5-HT_{1B} receptor (PDB code: 6G79) [25]. The results of molecular modeling were shown in Figure 2. The protonated nitrogen atom of **13m** formed a strong salt bridge with D3.32 in 5HT_{1A}R. The NH group of the indole ring formed hydrogen bonding with T3.37. The N-(cyclopropylmethyl)sulfamoyl moiety interacted with A2.61, Y2.64 and F3.28 through hydrophobic packing, which was in accordance with the binding mode of **FW01** with 5-HT_{1A}R. The isobutoxy group was inserted into another hydrophobic pocket formed by F6.51, V6.54 and I7.38.

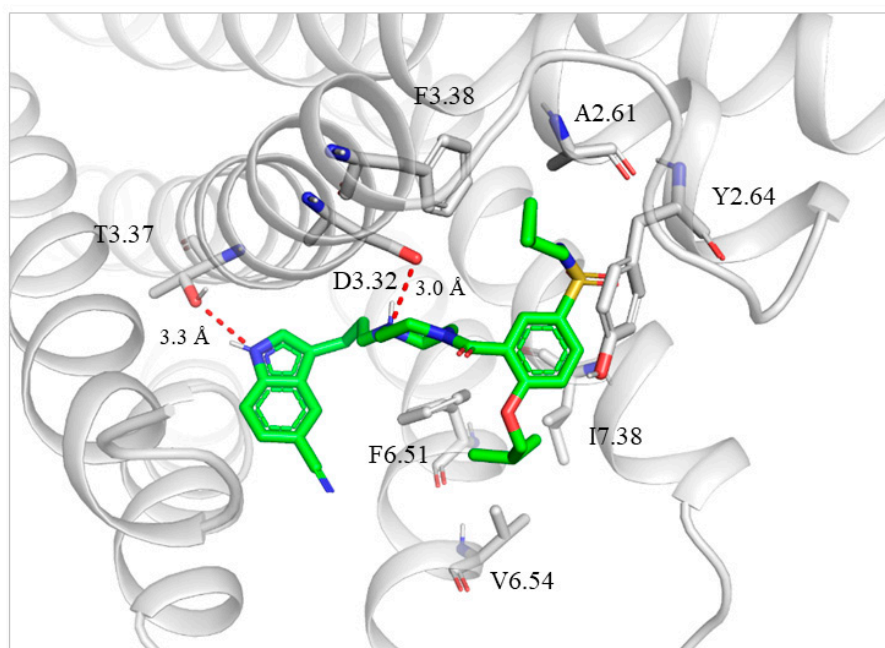


Figure 2. Binding mode of **13m** with 5-HT_{1A}R. The ligand is shown as green sticks. 5-HT_{1A}R and the surrounding residues are in gray. Hydrogen bond interactions are represented as dotted red lines.

To explain the high selectivity of **13m** toward 5-HT_{1A}R, the sequences of 5-HT_{1A}R, 5-HT_{2A}R and D₂R at the binding site were aligned. As shown in Figure 3A, the residues of the active site in three receptors differed greatly and thus the conformations of the three receptors at the binding site were different. The 3D structures of **13m**-bound 5-HT_{1A}R and 5-HT_{2A}R were superimposed to explain the selectivity of **13m** for 5-HT_{1A}R and 5-HT_{2A}R. The PDB code of 5-HT_{2A}R was 6A93 [26]. As shown in Figure 3B, compared with 5-HT_{1A}R, the amino acid residues in the hydrophobic pocket of 5-HT_{2A}R stretched out further. Thus the N-(cyclopropylmethyl)sulfamoyl of **13m** collapsed with W3.28 in the active pocket of 5-HT_{2A}R, which is obvious to be observed in Figure 3C. It accounted for the reduced affinity of **13m** for 5-HT_{2A}R. The same phenomenon was found in the case of D₂R when superposing 5-HT_{1A}R and D₂R (Figure 3D). The PDB code of D₂R was 6CM4 [27]. The amino acid residues in the active pocket of D₂R stretched out further than those in the active pocket of 5HT_{1A}R. Thus the indole head and the N-(cyclopropylmethyl)sulfamoyl of **13m** collapsed with S5.42 and L2.64 in the active pocket of D₂R. This explains why **13m** showed high selectivity toward 5-HT_{1A}R over 5-HT_{2A}R and D₂R.

2.5. *13m* Induced Activation Mechanism of 5-HT_{1A}R

Molecular dynamic simulations were carried out to explore the activation process of 5-HT_{1A}R by **13m**. Two systems, **13m** bound to the active-state 5-HT_{1A}R and the inactive-state 5-HT_{1A}R without ligand (apo), were performed for 200 ns simulation, respectively. The inactive-state 5-HT_{1A}R was modelled from the X-ray structure of 5-HT_{1B}R (PDB code: 5V54). The Gromos conformational cluster analysis was used to obtain the representative structures of two systems in the course of simulation.

In **13m**-5-HT_{1A}R system, a conserved hydrogen bond was formed between the NH group of the indole ring in **13m** and the oxygen atom of hydroxyl in T3.37 during the simulation (Figure 4A,D). At the same time, the protonated nitrogen atom in **13m** maintained a stable hydrogen bond with the carbonyl oxygen of D3.32 and a relatively weak interaction with the hydroxyl oxygen of Y7.43 (Figure 4B). Therefore, the interaction between D3.32 and Y7.43 (also called 3-7 lock) stayed unbroken in **13m**-5-HT_{1A}R system but experienced big fluctuation in apo system (Figure 4C). This phenomenon was in agreement with the previous study of our group [28]. The oxygen atom on the sulfonyl group

of **13m** formed a hydrogen bond with Q2.65 initially, but it fluctuates greatly due to the swing of the molecular tail after 80 ns (Figure 4E).

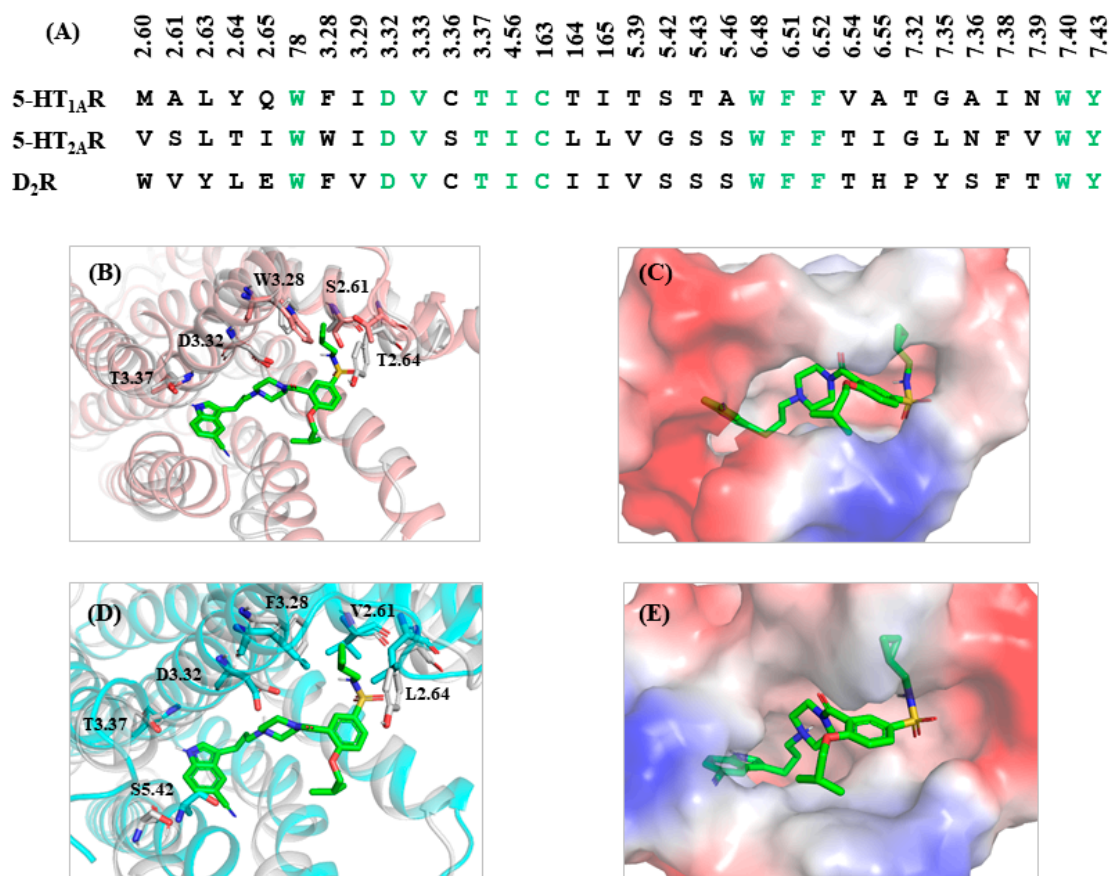


Figure 3. (A) Sequences of 5-HT_{1A}R, 5-HT_{2A}R, and D₂R at the binding site. (B) The superimposition of 5-HT_{2A}R with **13m**-bound 5-HT_{1A}R. (C) Electrostatic potential energy diagram of **13m** and 5-HT_{2A}R at the binding site. (D) The superimposition of D₂R with **13m**-bound 5-HT_{1A}R. (E) Electrostatic potential energy diagram of **13m** and D₂R at the binding site. The ligand is shown as green sticks. 5-HT_{1A}R and the surrounding residues are in gray. 5-HT_{2A}R and the surrounding residues are in pink. D₂R and the surrounding residues are in blue.

The strong interaction between **13m** and 5-HT_{1A}R induced the movement of TM3, TM5 and TM6. The triplets P5.50, I3.40 and F6.44 were located under the binding pockets of small molecules, their arrangement was important for stabilizing the antagonistic conformation of 5-HT_{1A}R. The interaction of **13m** with D3.32 and T3.37 adjusted the side chain of I3.40 to flip up, subsequently leading to the relocation of P5.50 and F6.44 (Figure 5A). Their rearrangement was closely related to the movement of the helices. At the same time, W6.48 moved outward due to the steric restraints between **13m** and residue W6.48. As a rotamer toggle switch, W6.48 further pushed the intracellular end of the TM6 to move inward and the external end of the TM6 to move outward (Figure 5B). Finally, TM3, TM5 and TM6 underwent large movement to create space for the binding of G_{α/s} protein (Figure 5C). It was worth noting that the TM6 moved outward 11.5 Å.

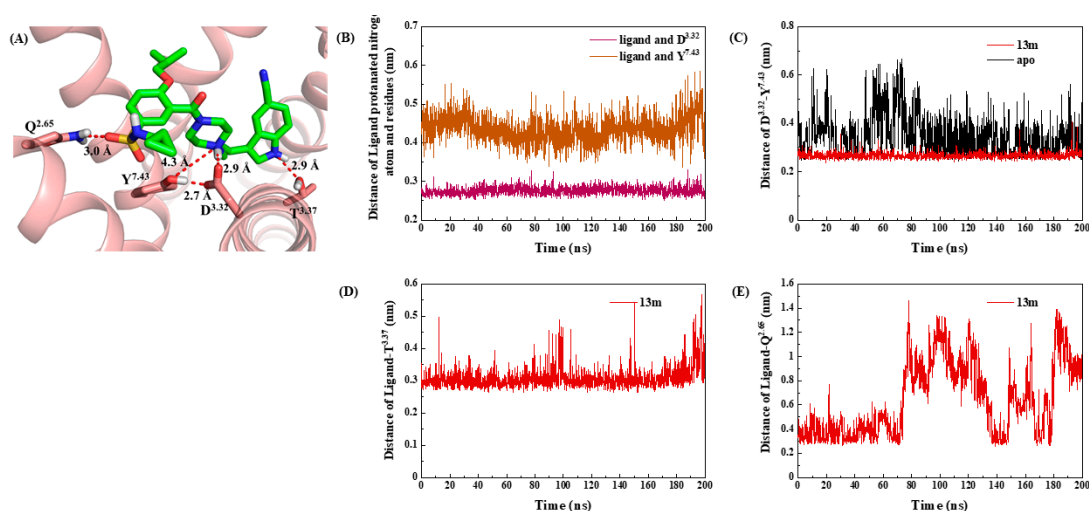


Figure 4. (A) The interaction between **13m** and D3.32, Y7.43, Q2.65 and T3.37. The ligand is shown as green sticks. 5-HT_{1A}R and the surrounding residues are in pink. Hydrogen bond interactions are represented as dotted red lines. (B) Distance of the ligand with D3.32 and Y7.43. (C) Distance between D3.32 and Y7.43. (D) Distance between ligand and T3.37. (E) The interaction between ligand and Q2.65 in **13m**-5-HT_{1A}R system.

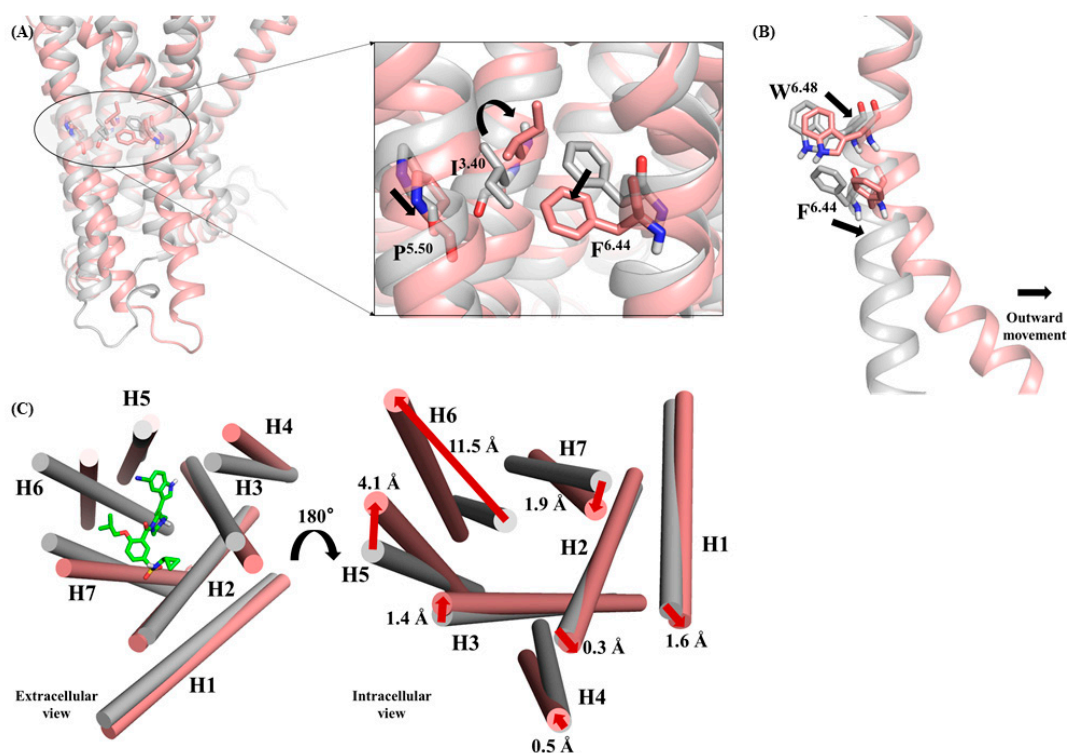


Figure 5. (A) Superimposed structures of apo and **13m**-5-HT_{1A}R systems and the rearrangements of I3.40, P5.50 and F6.44 when **13m** was bound to 5-HT_{1A}R. (B) the movement of rotamer toggle switch W6.48 in **13m**-5-HT_{1A}R system contributed to the movement of the TM6. (C) Superimposed structures of apo and **13m**-5-HT_{1A}R systems and the rearrangements of I3.40, P5.50, and F6.44 when **13m** was bound to 5-HT_{1A}R. The apo system and surrounding residues are represented as grey. The **13m**-5-HT_{1A}R system and surrounding residues are represented as pink.

On the basis of simulation trajectory and analysis results, a possible activation process of 5-HT_{1A}R could be proposed (Figure 6). Typically, unbound 5-HT_{1A}R maintained in an inactive state or a

basic active state. Owing to the intramolecular interaction and inherent flexibility, the molecular thermodynamic motion would lead to the dynamic equilibrium of several energy minima conformations of 5-HT_{1A}R. When **13m** got close to the binding pocket of 5-HT_{1A}R, the electrostatic effect between them promoted the ligand recognition and binding process. Then, **13m** stably stayed in the pocket enclosed by TM3, TM5, TM6 and TM7 through several anchoring interactions with the residues D3.32, Q2.65 and T3.37. These residues played the role of molecular triggers, propagating the conformational changes to the inner-middle part of the seven helices. The conformational changes induced the rearrangement of P5.50, I3.40 and F6.44 as well as the adjustment of W6.48, ultimately leading to the outward movement of TM3 and TM6, along with TM5 getting closer to TM6.

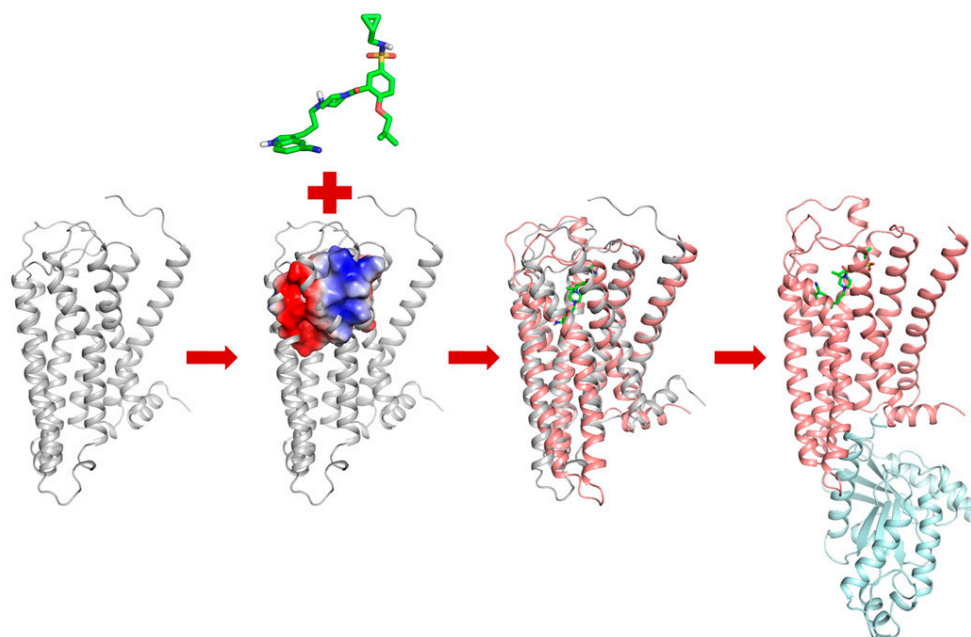


Figure 6. Proposed activation process of 5-HT_{1A}R. The apo system and surrounding residues are represented as grey. The **13m**-5-HT_{1A}R system and surrounding residues are represented as pink. The G_{α/s} protein is represented as blue.

The synergic helix movement of TM3, TM5, and TM6 created space for the binding of G_{α/s} protein. Then, 5-HT_{1A}R was fully activated, subsequently leading to the downstream signal transduction.

3. Experiment Protocols

3.1. Chemistry and Biological Evaluation

The compound synthesis methods, NMR data and biological evaluation methods were provided in the Supplementary Materials.

3.2. Molecular Modeling

3.2.1. Homology Modeling

The amino acid sequence of 5-HT_{1A}R were downloaded from the UniProtKB database (Entry code: P08908), and sequence similarity search was performed using NCBI BLAST server (Bethesda, MD, USA) [29]. The structure (PDB code: 6G79 and 5V54) of 5-HT_{1B} receptor were selected as the templates to construct the agonistic and antagonistic conformation of 5-HT_{1A} receptor. Sequence alignment of 5-HT_{1B} receptor and 5-HT_{1A}R was carried out using Discovery Studio 2016 (hereafter abbreviated to DS) (Waltham, MA, USA). Homology modeling was performed with DS. Ten models were generated after loop refinement and the one with the lowest Discrete Optimized Protein Energy (DOPE) score

was submitted to energy minimization (100 steps steepest descent with backbone constrained). The PROCHECK program (Cambridge, UK) was used to evaluate the stereochemical quality of 5-HT_{1A}R [30].

3.2.2. Molecular Docking Operations

Molecular docking was carried out using GOLD 5.0.1 (Cambridge, UK). The binding site was defined to include all residues within a 15.0 Å radius of the conserved D3.32 C γ carbon atom of 5-HT_{1A}R. Ten conformations were produced for each ligand, and Gold-Score was used as scoring function. Other parameters were set as standard default. High-scoring complexes were inspected visually to identify the most reasonable solution.

3.3. Molecular Dynamic Simulations

The molecular dynamic (MD) simulations were performed using the GROMACS 5.1.2 package (Uppsala, Sweden) [31]. Two systems, **13m** bound to active-state 5-HT_{1A}R and inactive-state 5-HT_{1A}R without ligand (apo), were embedded in the hydrated, equilibrated palmitoylcholine phosphatidylcholine (POPC) bilayer via the CHARMM-GUI server. The TIP3P water model was used for the MD simulation. Sodium and chloride ions were added to neutralize two systems to an ionic concentration of 0.15 mol/L. Both systems were minimized and gradually equilibrated in an NPT ensemble at 310 K and 1 bar. Periodic boundary conditions were applied to these simulation systems. Bonds connected to hydrogen atoms were restrained with the LINCS algorithm to allow an integration time step of 2 fs. Electrostatic interactions were calculated using the particle mesh Ewald (PME) method. Finally, the MD simulations for both systems were performed for 200 ns. All analysis of MD trajectories was performed using tools implemented in the GROMACS 5.1.2 package (Uppsala, Sweden). All the structural graphics were processed with PyMOL software (San Carlos, CA, USA) [32].

4. Conclusions

In summary, a series of indolealkylpiperazine derivatives with a benzamide moiety were designed and synthesized. Their activities on dopamine and serotonin receptors were evaluated and these compounds were found to be selective 5-HT_{1A}R agonists. Among all tested compounds, **13m** displayed the most potent agonistic activity over 5-HT_{1A}R with an EC₅₀ value of 1.01 nM. The investigation of the binding mode uncovered the mechanism of **13m**'s potent agonistic activity and high selectivity. In addition, molecular dynamic simulations were carried out to propose **13m** induced activation model of 5-HT_{1A}R. The electrostatic interaction between the negatively charged active site of the 5-HT_{1A}R and the positively protonated charged **13m** is the initial driving force for the ligand recognition. **13m** formed anchoring interactions with residues D3.32, Q2.65, T3.37 and induced conformation changes of 5-HT_{1A}R. This leads to the rearrangement of P5.50, I3.40 and F6.44 as well as the adjustment of W6.48, causing the outward movement of TM3 and TM6, along with TM5 getting closer to TM6. Then, 5-HT_{1A}R was ready to bind G α /_s protein, leading itself to a fully activated state. This model would further promote structure-based agonist design of 5-HT_{1A}R for the treatment of depression.

Supplementary Materials: The following are available online, the compound synthesis methods, NMR data, biological evaluation methods.

Author Contributions: C.Z., X.L. and W.P. contributed equally in this work. Compound design, C.Z. and W.F.; compound synthesis, C.Z., X.L. and W.P.; writing—original draft preparation, C.Z. and X.L.; writing—review and editing, W.F.; funding acquisition, W.F. All authors have read and agreed to the published version of the manuscript.

Funding: This work is supported by grants from National Natural Science Foundation of China (NO. 81773635, NO. 82073765) and Shanghai Science and Technology Development Funds (14431900500, 20S11902400).

Conflicts of Interest: The authors declare no conflict of interest.

References

1. De Oliveira, M.R.; Chenet, A.L.; Duarte, A.R.; Scaini, G.; Quevedo, J. Molecular Mechanisms Underlying the Anti-depressant Effects of Resveratrol: A Review. *Mol. Neurobiol.* **2017**, *55*, 4543–4559. [[CrossRef](#)] [[PubMed](#)]
2. Cui, R. Editorial (Thematic Selection: A Systematic Review of Depression). *Curr. Neuropharmacol.* **2015**, *13*, 480. [[CrossRef](#)] [[PubMed](#)]
3. Hawton, K.; I Comabella, C.C.; Haw, C.; Saunders, K.E.A. Risk factors for suicide in individuals with depression: A systematic review. *J. Affect. Disord.* **2013**, *147*, 17–28. [[CrossRef](#)] [[PubMed](#)]
4. Rihmer, Z. Antidepressants, depression and suicide. *Neuropsychopharmacol. Hung.* **2013**, *15*, 157–164.
5. Lacerda-Pinheiro, S.F.; Junior, R.F.F.P.; De Lima, M.A.P.; Da Silva, C.G.L.; Dos Santos, M.D.S.V.; Júnior, A.G.T.; De Oliveira, P.N.L.; Ribeiro, K.D.B.; Neto, M.L.R.; Bianco, B. Are there depression and anxiety genetic markers and mutations? A systematic review. *J. Affect. Disord.* **2014**, *168*, 387–398. [[CrossRef](#)] [[PubMed](#)]
6. Vrijzen, J.N.; Van Oostrom, I.; Franke, B.; Becker, E.S.; Speckens, A.; Arias-Vásquez, A. Association between genes, stressful childhood events and processing bias in depression vulnerable individuals. *Genes Brain Behav.* **2014**, *13*, 508–516. [[CrossRef](#)]
7. Latendresse, G.; Elmore, C.; Deneris, A. Selective Serotonin Reuptake Inhibitors as First-Line Antidepressant Therapy for Perinatal Depression. *J. Midwifery Women's Health* **2017**, *62*, 317–328. [[CrossRef](#)]
8. Mago, R.; Mahajan, R.E.; Thase, M. Levomilnacipran: A newly approved drug for treatment of major depressive disorder. *Expert Rev. Clin. Pharmacol.* **2014**, *7*, 137–145. [[CrossRef](#)]
9. Kornstein, S.G.; McIntyre, R.S.; Thase, M.E.; Boucher, M. Desvenlafaxine for the treatment of major depressive disorder. *Expert Opin. Pharmacother.* **2014**, *15*, 1449–1463. [[CrossRef](#)]
10. Yoshinaga, H.; Nishida, T.; Sasaki, I.; Kato, T.; Oki, H.; Yabuuchi, K.; Toyoda, T. Discovery of DSP-1053, a novel benzylpiperidine derivative with potent serotonin transporter inhibitory activity and partial 5-HT_{1A} receptor agonistic activity. *Bioorganic Med. Chem.* **2018**, *26*, 1614–1627. [[CrossRef](#)]
11. Seabrook, E.; Kern, M.L.; Rickard, N.S.; Cha, M.; Rice, S.; Gritton, J. Social Networking Sites, Depression, and Anxiety: A Systematic Review. *JMIR Ment. Health* **2016**, *3*, e50. [[CrossRef](#)] [[PubMed](#)]
12. Cowen, P.J. Backing into the future: Pharmacological approaches to the management of resistant depression. *Psychol. Med.* **2017**, *47*, 2569–2577. [[CrossRef](#)] [[PubMed](#)]
13. Penn, E.; Tracy, D.K. The drugs don't work? Antidepressants and the current and future pharmacological management of depression. *Ther. Adv. Psychopharmacol.* **2012**, *2*, 179–188. [[CrossRef](#)] [[PubMed](#)]
14. Marston, O.J.; Garfield, A.S.; Heisler, L.K. Role of central serotonin and melanocortin systems in the control of energy balance. *Eur. J. Pharmacol.* **2011**, *660*, 70–79. [[CrossRef](#)] [[PubMed](#)]
15. Berger, M.; Gray, J.A.; Roth, B.L. The Expanded Biology of Serotonin. *Annu. Rev. Med.* **2009**, *60*, 355–366. [[CrossRef](#)] [[PubMed](#)]
16. Nichols, D.E.; Nichols, C.D. Serotonin Receptors. *Chem. Rev.* **2008**, *108*, 1614–1641. [[CrossRef](#)] [[PubMed](#)]
17. Czopek, A.; Byrtus, H.; Kolaczowski, M.; Pawłowski, M.; Dybała, M.; Nowak, G.; Tatarczynska, E.; Wesołowska, A.; Chojnacka-Wójcik, E. Synthesis and pharmacological evaluation of new 5-(cyclo)alkyl-5-phenyl- and 5-spiroimidazolidine-2,4-dione derivatives. Novel 5-HT_{1A} receptor agonist with potential antidepressant and anxiolytic activity. *Eur. J. Med. Chem.* **2010**, *45*, 1295–1303. [[CrossRef](#)]
18. Shimizu, S.; Tataru, A.; Imaki, J.; Ohno, Y. Role of cortical and striatal 5-HT_{1A} receptors in alleviating antipsychotic-induced extrapyramidal disorders. *Prog. Neuro-Psychopharmacol. Biol. Psychiatry* **2010**, *34*, 877–881. [[CrossRef](#)]
19. Blier, P.; Ward, N.M. Is There A Role for 5-HT_{1A} Agonists in the Treatment of Depression? *Biol. Psychiatry* **2003**, *53*, 193–203. [[CrossRef](#)]
20. Bara-Jimenez, W.; Bibbiani, F.; Morris, M.J.; Dimitrova, T.; Sherzai, A.; Mouradian, M.M.; Chase, T.N. Effects of serotonin 5-HT_{1A} agonist in advanced Parkinson's disease. *Mov. Disord.* **2005**, *20*, 932–936. [[CrossRef](#)]
21. Blier, P.; De Montigny, C. Current advances and trends in the treatment of depression. *Trends Pharmacol. Sci.* **1994**, *15*, 220–226. [[CrossRef](#)]
22. Xu, L.; Zhou, S.; Yu, K.; Gao, B.; Jiang, H.; Zhen, X.; Fu, W. Molecular Modeling of the 3D Structure of 5-HT_{1A}R: Discovery of Novel 5-HT_{1A}R Agonists via Dynamic Pharmacophore-Based Virtual Screening. *J. Chem. Inf. Model.* **2013**, *53*, 3202–3211. [[CrossRef](#)] [[PubMed](#)]

23. Heinrich, T.; Böttcher, H.; Gericke, R.; Bartoszyk, G.D.; Anzali, S.; Seyfried, C.A.; Greiner, H.E.; Van Amsterdam, C. Synthesis and Structure–Activity Relationship in a Class of Indolebutylpiperazines as Dual 5-HT_{1A} Receptor Agonists and Serotonin Reuptake Inhibitors. *J. Med. Chem.* **2004**, *47*, 4684–4692. [[CrossRef](#)] [[PubMed](#)]
24. Lian, P.; Li, L.; Geng, C.; Zhen, X.; Fu, W. Higher-Affinity Agonists of 5-HT_{1A}R Discovered through Tuning the Binding-Site Flexibility. *J. Chem. Inf. Model.* **2015**, *55*, 1616–1627. [[CrossRef](#)]
25. García-Nafria, J.; Nehmé, R.; Edwards, P.C.; Tate, C.G. Cryo-EM structure of the serotonin 5-HT_{1B} receptor coupled to heterotrimeric Go. *Nature* **2018**, *558*, 620–623. [[CrossRef](#)]
26. Kimura, K.T.; Asada, H.; Inoue, A.; Kadji, F.M.N.; Im, D.; Mori, C.; Arakawa, T.; Hirata, K.; Nomura, Y.; Nomura, N.; et al. Structures of the 5-HT_{2A} receptor in complex with the antipsychotics risperidone and zotepine. *Nat. Struct. Mol. Biol.* **2019**, *26*, 121–128. [[CrossRef](#)]
27. Wang, S.; Che, T.; Levit, A.; Shoichet, B.K.; Wacker, D.; Roth, B.L. Structure of the D₂ dopamine receptor bound to the atypical antipsychotic drug risperidone. *Nature* **2018**, *555*, 269–273. [[CrossRef](#)]
28. Wang, W.; Zheng, L.; Li, W.; Zhu, C.; Peng, W.; Han, B.; Fu, W. Design, Synthesis, and Structure–Activity Relationship Studies of Novel Indolylalkylpiperazine Derivatives as Selective 5-HT_{1A} Receptor Agonists. *J. Chem. Inf. Model.* **2020**, *60*, 235–248. [[CrossRef](#)]
29. Johnson, M.; Zaretskaya, I.; Raytselis, Y.; Merezuk, Y.; McGinnis, S.; Madden, T.L. NCBI BLAST: A better web interface. *Nucleic Acids Res.* **2008**, *36*, w5–w9. [[CrossRef](#)]
30. Laskowski, R.A.; MacArthur, M.W.; Moss, D.S.; Thornton, J.M. PROCHECK—A program to check the stereochemical quality of protein structures. *J. Appl. Cryst.* **1993**, *26*, 283–291. [[CrossRef](#)]
31. Hess, B.; Kutzner, C.; van der Spoel, D.; Lindahl, E. GROMACS 4: Algorithms for Highly Efficient, Load-Balanced, and Scalable Molecular Simulation. *J. Chem. Theory Comput.* **2008**, *4*, 435–447. [[CrossRef](#)] [[PubMed](#)]
32. DeLano, W.L. *The PyMOL Molecular Graphics System*, version 1.2r3pre; Schrödinger, LLC.: San Carlos, CA, USA, 2002; 3p.

Sample Availability: Samples of the compounds are available from the authors.

Publisher’s Note: MDPI stays neutral with regard to jurisdictional claims in published maps and institutional affiliations.



© 2020 by the authors. Licensee MDPI, Basel, Switzerland. This article is an open access article distributed under the terms and conditions of the Creative Commons Attribution (CC BY) license (<http://creativecommons.org/licenses/by/4.0/>).